Received: 4 September 2024 | Revised: 4 December 2024 | Accepted: 16 December 2024

DOI: 10.1111/ppl.70146

ORIGINAL RESEARCH

Physiologia Plantarum

Differential gene expression and metabolic pathways in *Toona sinensis*: Influence on colour and aroma

Rui Zeng[1,2] | Mingmin Zheng[1,2] | Yunhong Gao[3] | Jianchun Hu[4] | Javed Ahmad[5] | Muhammad Umer Farooq[5] | Songqing Liu[1,2] | Xiangmei Lin[1] | Suleyman I. Allakhverdiev[6,7] | Sergey Shabala[8,9]

[1]College of Chemistry and Life Science, Chengdu Normal University, Chengdu, Sichuan, China

[2]Sichuan Provincial Key Laboratory for Development and Utilization of Characteristic Horticultural Biological Resources, College of Chemistry and Life Sciences, Chengdu Normal University, Chengdu, China

[3]Sichuan Yizhong Agricultural Development Co., Ltd, Chengdu, China

[4]Xichang University, Xichang, China

[5]Wheat Research Institute, Ayub Agricultural Research Institute Faisalabad, Punjab, Pakistan

[6]K.A. Timiryazev Institute of Plant Physiology, Russian Academy of Sciences, Moscow, Russia

[7]Faculty of Engineering and Natural Sciences, Bahcesehir University, Istanbul, Turkey

[8]School of Biological Science, University of Western Australia, Crawley, Australia

[9]International Research Centre for Environmental Membrane Biology, Foshan University, Foshan, China

Correspondence
Rui Zeng,
Email: zengrui829@126.com

Sergey Shabala,
Email: sergey.shabala@uwa.edu.au

Funding information
Chengdu Normal University, Grant/Award Numbers: 2023JG19, YJRC2021-03

Edited by B. Huang

Abstract

Toona sinensis, a plant species renowned for its culinary and medicinal properties, exhibits diverse colour variations that contribute to its aesthetic appeal and commercial value. Understanding the molecular mechanisms underlying colour and aroma traits in *Toona sinensis* is crucial for breeding programs and quality regulation in agriculture and the food industry. The present investigation included a comprehensive analysis of the transcriptomic and metabolomic profiles of *Toona sinensis* with different colours, including green, red, and red leaves with green stems. Metabolic analysis revealed that the flavonoid biosynthesis pathway governs the colour distinction between green and red *Toona sinensis*. The top 10 metabolites influenced by transcriptome include terpenoids (5), heterocyclic compounds (1), phenol (1), ketone (1), aldehyde (1), and alcohol (1). Fifteen highly expressed genes impacted by phenylpropanoid, sesquiterpenoid, and triterpenoid biosynthesis in coloured *Toona sinensis*. Functional annotation and pathway analysis revealed that terpene metabolites are predominantly synthesized via terpene metabolic pathway, involving eight key gene families. This study underscores the importance of multi-omics approaches in unravelling the genetic and metabolic basis of phenotypic traits in plant species aimed at improving colour, aroma, and nutritional quality in plants and derived products.

Highlights

- Flavonoid biosynthesis pathway governs the colour distinction between green and red *Toona sinensis*.
- The top 10 metabolites influenced by transcriptome include five terpenoids, one heterocyclic compound, one phenol, one ketone, one aldehyde, and one alcohol.
- Fifteen highly expressed genes impacted by phenylpropanoid, sesquiterpenoid, and triterpenoid biosynthesis in coloured *Toona sinensis*.

- Terpene metabolites are predominantly synthesized via the terpene metabolic pathway, involving eight key gene families.
- The net photosynthetic rate and intercellular CO_2 concentration are relatively high in the red *Toon sinensis* morph.

1 | INTRODUCTION

Toona sinensis (commonly called Toon) is a deciduous tree from the Meliaceae family. It is uniquely regarded as a vegetable worldwide and has multiple aesthetic, nutritional and medicinal impacts, further, it is traditionally used in various products (Jiang et al., 2019). Toon is the predominant variety of China's "forest vegetables" and is renowned for its distinct flavour and aroma characteristics. The plant's ecology is greatly determined by the organs like leaves (Petit Bon et al., 2020). There are several native breeds of *Toona sinensis*, such as red *Toona sinensis*, red oil *Toona sinensis*, black oil *Toona sinensis*, and green *Toona sinensis*, earning it the moniker of a peculiar "tree lettuce". *Toona sinensis* is a collective term for these varieties, which are rare, distinctive, and concurrently used as a medicinal and edible new-type vegetable (Zhao et al., 2022). Toon is rich in nutrients like vitamin C, high-quality protein, phosphorus, and iron minerals (Zhai, 2020). Beyond its nutritional value and pleasant taste, it offers significant health benefits and antioxidant properties, including the removal of harmful substances from the human body (Yang et al., 2011, Yu et al., 2012). It also exhibits antibacterial, antiviral (Chen et al., 2008), anti-inflammatory, and immunomodulatory effects (Lim et al., 2020) due to the bioactive functional compounds like flavonoids, phenols, and terpenoids. Like other plants in the Meliaceae family, the main components of the Chinese toon are terpenes, including triterpenoids (gansuline, limonoids, norlimonoids), diterpenes and sesquiterpenes (Peng et al., 2019).

In nature, plants emit a vast array of volatile organic compounds (VOCs), which are integral to their chemotype and play a central role in plant ecosystems as ecological signals. Over 1,700 compounds have been categorized as VOCs of plant origin (Dudareva et al., 2013). The biosynthetic nature of these compounds classifies them as (1) terpenoids, (2) volatile oil, (3) phenylpropanoids, (4) flavonoids, (5) benzene ring and phenylpropane derivatives, (6) fatty acid and amino acid derivatives, along with some special substances such as sulfur and nitrogen compounds. The synthesis of plant VOCs occurs during the physiological and metabolic processes of various tissues and organs, primarily being released into the air through leaves. There are noticeable variations in the composition of VOCs released by different plant species. In flowers and fruits, the VOCs synthesized and released are mainly aromatic compounds, terpenoids, and esters (Wei et al., 2016; Du et al., 2019; Xia et al., 2021). Conversely, in leaves, terpenoids and fatty acid derivatives predominate, with the occasional presence of nitrogenous compounds like indole (Song et al., 2020, Wang et al., 2021) serving these purposes. Numerous studies have highlighted the high specificity of plant VOCs for different plant species, emphasizing their critical roles in signal transduction (Chen et al., 2020), biotic and abiotic stress tolerance (Holopainen & Gershenzon, 2010), and biotic interactions (Kalske et al., 2019).

Studies have identified terpenes and sulfur-containing compounds, along with a small number of aldehydes, alcohols, and alkanes, as the substances responsible for the distinctive aroma of *Toona sinensis* shoots (Liu et al., 2013; Wu et al., 2014; Peng et al., 2019; Jiang et al., 2020). While some studies have revealed the genome composition, evolutionary relationships, and related pathways of terpenoid biosynthesis in *Toona sinensis* (Ji et al., 2021), the biosynthesis pathways and molecular mechanisms of its aroma constituents are still poorly understood.

High-throughput sequencing has proven successful in elucidating gene function in non-model plants, allowing for a comprehensive understanding of the genome, transcriptome, and metabolome, as well as the interpretation of regulatory networks within species. Also, the integration of transcriptomics and metabolomic data through weighted gene co-expression network analysis (WGCNA) has emerged as an effective method for discovering novel gene functions and unveiling intricate co-expression networks that regulate secondary metabolism (Langfelder & Horvath, 2008; Pei et al., 2017). This approach has been applied to research on various plants, including Zanthoxylum (Fei et al., 2021), fig (Borges et al., 2013), daffodil (Yang et al., 2021), jasmine (Zhou et al., 2022), and others shedding light on the aroma mechanisms of these species.

Flavour stands as a crucial quality attribute in food, serving as a significant determinant for consumers when making purchasing decisions. Presently, the characteristic flavour of Toon is perceived as volatile and unstable, with a complex aroma composition. Moreover, the leaf colour of Toon is notably influenced by the light environment, leading to distinct odour variations among Toons of different colours.

In this study, we report aroma-related metabolites across various coloured Toon, and variations in their composition and content. Additionally, comparative genomic analysis of metabolites and transcriptomes was conducted through homolog alignment and integration, facilitating the identification of candidate genes associated with aroma in Toon. We also constructed a transcriptional regulatory network, providing essential insights for the subsequent functional verification of related genes and establishing a foundation for quality breeding and regulation of Toon. The findings of this work are essential for a better understanding of the complex interplay between gene expression, metabolite composition, and phenotype in *Toona sinensis* and could be extrapolated to other species.

2 | MATERIALS AND METHODS

2.1 | Materials

The *Toona sinensis* (Toona) samples were triplicated and grown outdoors throughout the seasons in 2022–23. Toons were harvested from Yaodu Town, Qingbai jiang District, Chengdu City, Sichuan Province (30°48′27.7″N, 104°19′58.5″E). Mature, first-crop, fresh, robust Toona buds that were free of diseases, insect pests, and mechanical damage were selected for experimental study. Forty-five Toon samples were selected. Three different coloured Toona morphs were collected: all red (R), red leaves and green stems (RG), and all green (G) (Figure S1). The notable high photosynthetic rate and intercellular CO_2 concentration in the red Toona morph were observed using the H-GH40 portable photosynthesis meter (Table S2). The materials (leaf and shoots) were weighed and stored using liquid nitrogen for further analysis at −80°C.

2.2 | Sample preparation and treatment

The Toona leaf samples were ground into powder using liquid nitrogen. 500 g (1 mL) of the powder was immediately transferred to a 20 mL headspace vial (Agilent) containing a saturated NaCl solution to prevent any enzymatic reaction. The vials were then sealed with TFE silicone headspace crimp caps (Agilent). During solid-phase microextraction (SPME) analysis, each vial was heated at 60°C for 5 min. Samples were then prepared for further analytical testing by exposing a 120 μm DVB/CWR/PDMS optical fiber (Agilent) to the headspace of the sample at 100°C for 15 min.

2.3 | Analysis of volatile organic compounds by SPME-GC–MS

The Agilent Model 8890 GC coupled with a 7000D mass spectrometer (Agilent) was utilized for the identification and quantification of volatile organic compounds (VOCs), as the latter determine plants' aroma. Following sampling, VOC desorption from the fiber coating occurred in the injection port of the GC apparatus (Model 8890; Agilent) for 5 minutes at 250°C in split-less mode. Equipped with a 30 m × 0.25 mm × 0.25 μm DB-5MS (5% phenyl-polymethylsiloxane) capillary column, the setup utilized helium as the carrier gas, flowing at a linear velocity of 1.2 mL min^{-1}. The injector temperature was held at 250°C, with the detector operating at 280°C.

The oven temperature was programmed as follows: initially set at 40°C for 3.5 minutes, then increased at 10°C min^{-1} to 100°C, followed by a ramp of 7°C min^{-1} to 180°C, and finally a ramp of 25°C min^{-1} to 280°C, with a 5-minute hold period. Mass spectra were recorded in electron impact (EI) ionization mode at 70 eV. The temperatures for the quadrupole mass detector, ion source, and transfer line were set at 150, 230, and 280°C, respectively. Selected ion monitoring (SIM) mode was employed by the MS for the identification and quantification of analytes. The identified compounds through GC–MS, including the chromatographic retention indices (RI) of each identified compound, are provided in Table S1.

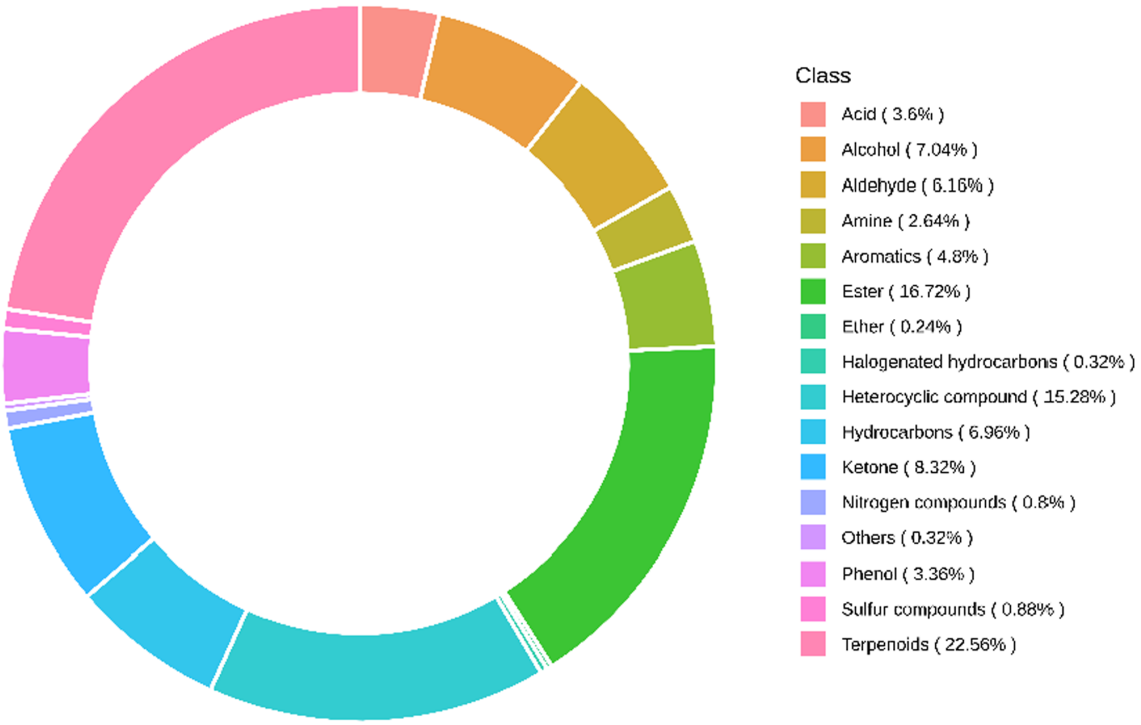

FIGURE 1 Metabolites class differentiation in *Toona sinensis*. Each color represents a metabolite class, and the patch area represents the proportion of metabolites in that class.

2.4 | RNA quantification and qualification

To monitor RNA degradation and contamination, 1% agarose gel electrophoresis was employed. The purity assessment of RNA was conducted using the Nano Photometer® spectrophotometer (IMPLEN). RNA concentration was determined with the Qubit® RNA Assay Kit on the Qubit®2.0 Fluorometer (Life Technologies). Evaluation of RNA integrity was carried out using the RNA Nano 6000 Assay Kit on the Bioanalyzer 2100 system (Agilent Technologies). For RNA sample preparations, 1 μg RNA per sample was used. Sequencing libraries were generated using the NEBNext® UltraTM RNA Library Prep Kit for Illumina® (NEB), following the manufacturer's protocol, with index codes added for sample attribution.

First, mRNA was isolated from total RNA using poly-T oligo-attached magnetic beads. Subsequently, fragmentation was achieved using divalent cations under elevated temperature in NEBNext First Strand Synthesis Reaction Buffer (5X). For first-strand cDNA synthesis, random hexamer primers and M-MuLV Reverse Transcriptase (RNase H-) were utilized. Second-strand cDNA synthesis was then carried out using DNA Polymerase I and RNase H. Any remaining overhangs were converted into blunt ends via exonuclease/polymerase activities. Finally, the adenylation of the 3′ ends of DNA fragments was performed, followed by ligation of NEBNext Adaptor with a hairpin loop structure to prepare for hybridization.

The library fragments, targeted to be within the range of 250–300 bp in length, underwent purification using the AMPure XP system (Beckman Coulter). Subsequently, 3 μL of USER Enzyme (NEB, USA) was applied to the size-selected, adaptor-ligated cDNA at 37°C for 15 min, followed by a 5-min incubation at 95°C prior to PCR. PCR was then conducted using Phusion High-Fidelity DNA polymerase, Universal PCR primers, and Index (X) Primer. Finally, the PCR products underwent purification using the AMPure XP system, and the quality of the library was evaluated using the Agilent Bioanalyzer 2100 system.

2.5 | Transcriptome analysis

The DESeq2 v1.22.1 was utilized to analyze the genes differential expression (DEGs) between the two groups (for samples with biological replicates). In cases where samples lacked biological replicates, differential analysis was conducted using edgeR. The Benjamini & Hochberg method was employed to determine corrected P values. The P value (corrected) and |log2foldchange| were used to determine significant differential expression.

Multiple databases were opted to estimate Gene function annotation and pathway analysis, including GO (Gene Ontology), KEGG (Kyoto Encyclopedia of Genes and Genomes), KOG/COG (COG: Clusters of Orthologous Groups of proteins; KOG: eukaryotic Ortholog Groups), Pfam (protein family), Swiss-Prot (a manually annotated and reviewed protein sequence database) and Nr (NCBI non-redundant protein sequences).

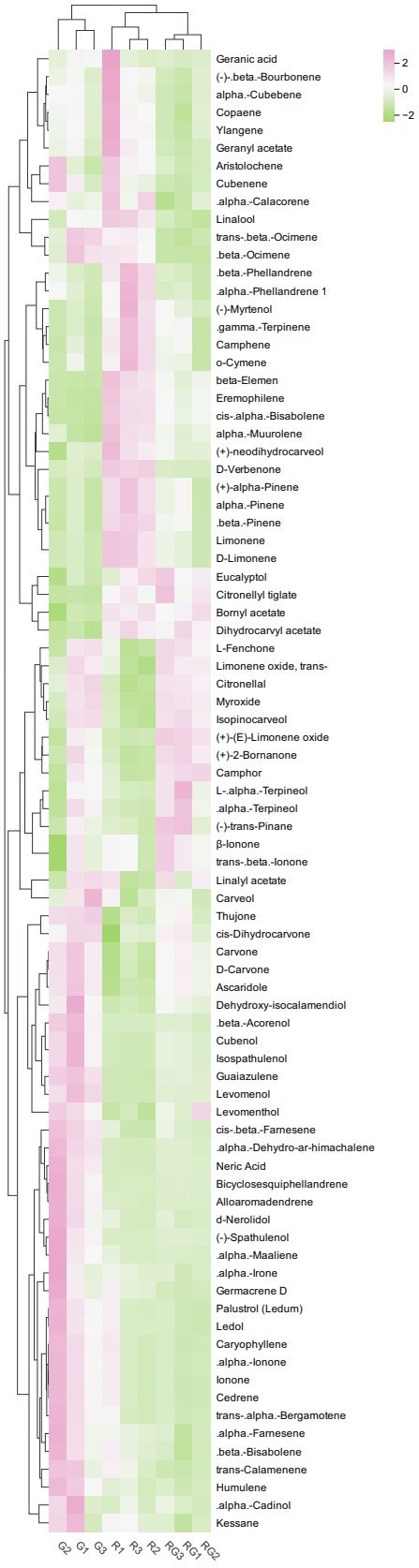

FIGURE 2 Heat map of individual terpenoid contents among different *Toona sinensis* morphs.

2.6 | Weighted gene co-expression network analysis (WGCNA)

Utilizing the Weighted Gene Co-expression Network Analysis (WGCNA) R Package (v1.69), the Weighted Correlation Network Analysis was conducted on the transcriptome data to identify highly coordinated gene sets during different *Toona sinensis* morphs, as well as associations between gene sets and aroma. Genes with FPKM >0.8 were used to construct a weighted gene co-expression network. This analysis aimed to identify highly coordinated gene sets within different coloured Toona sinensis.

2.7 | Statistical analyses

The significant differences were determined by ANOVA and Duncan's multiple range test ($p < 0.05$) using DPS 7.05 during the analysis of the experimental data.

3 | RESULTS

3.1 | The volatile organic compounds (VOCs) differences in different coloured Toona sinensis

Gas chromatography–mass spectrometry (GC–MS) was employed to measure the VOCs content differences in Toon material under investigation. The metabolic analysis identified a total of 1251 metabolites in this study, encompassing terpenes (22.6%), esters (16.7%), heterocyclic compounds (15.3%), ketones (8.3%), alcohols (7.04%), hydrocarbons (6.96%), aldehyde (6.2%), aromatics (4.8%), organic acids (3.6%), phenols (3.4%), amines (2.64%), and other (Figure 1). The Orthogonal Partial Least Squares Discriminant Analysis (OPLS-DA) results indicated substantial differences between the sample groups (R, G, RG), while the variations within the groups were minimal. Copaene was the most abundant terpenoid in red *Toona sinensis*, whereas L-α-terpineol was the most abundant terpenoid in RG *Toona sinensis*, and α-ionone was the most abundant terpenoid in green *Toona sinensis*. Monoterpenes

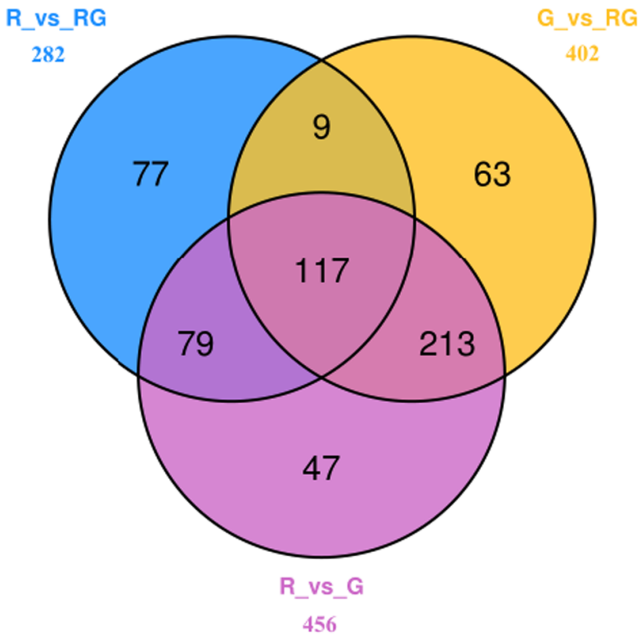

FIGURE 4 A Venn diagram of metabolites categorization among different *Toona sinensis* morphs.

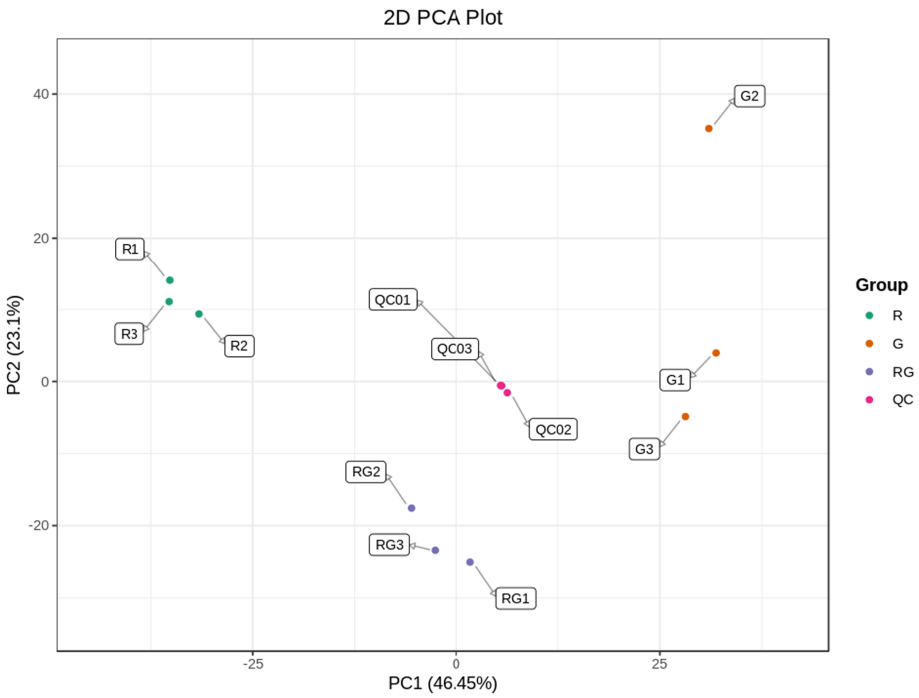

FIGURE 3 2D-PCA score plot of mass spectra data for each group of samples and QC samples. PC1 represents the first principal component, PC2 represents the second principal component. The percentage represents the interpretation rate of the principal component to the data set.

and sesquiterpenes were the main terpenoid components of different *Toona sinensis* morphs (Figure 2).

Using GC–MS data coupled with principal component analysis (PCA), a comparison was made of the metabolite composition involved in the fruit development of Toon. The results disclosed distinct separations in the metabolite compositions in the samples studied (R, RG, G). The PC1 × PC2 score plots were found to represent the main characteristics of the samples (Figure 3). Based on a significant eigenvalue, PCs were identified. The significant PCs accounting for total variability were 46.5% (PC1) and 23.1% (PC2). The PCA method effectively discriminated against R, G, and RG. The first quadrant was highly related to the G and quality control group (QC), which represented a strong correlation between them. The RG group was mainly inclined to the 2nd and 3rd quadrants. However, the R group was found to reside in the 4th Quadrant.

We identified a total of 1140 differential metabolites. Each circle indicates the total number of metabolites that exist in each respective group, while the overlapping regions represent the number of metabolites shared between those groups. The metabolites that reside in the G group were notably higher than in the R and RG groups (Figure 4). The R_vs_RG metabolic model contains a total of 282 unique metabolites, and the G_vs_RG identified a total of 402 metabolites, while there are a total of 456 metabolites tested in R_vs_G group with 117 shared metabolites.

The classification of metabolites between different Toon groups was further accessed to identify their up- and down-regulation. Between the R and RG groups, the expression of 189 metabolites increased, while 57 decreased; 1001 were expressed insignificantly. In G and RG groups, 151 metabolites increased, and 93 decreased, while

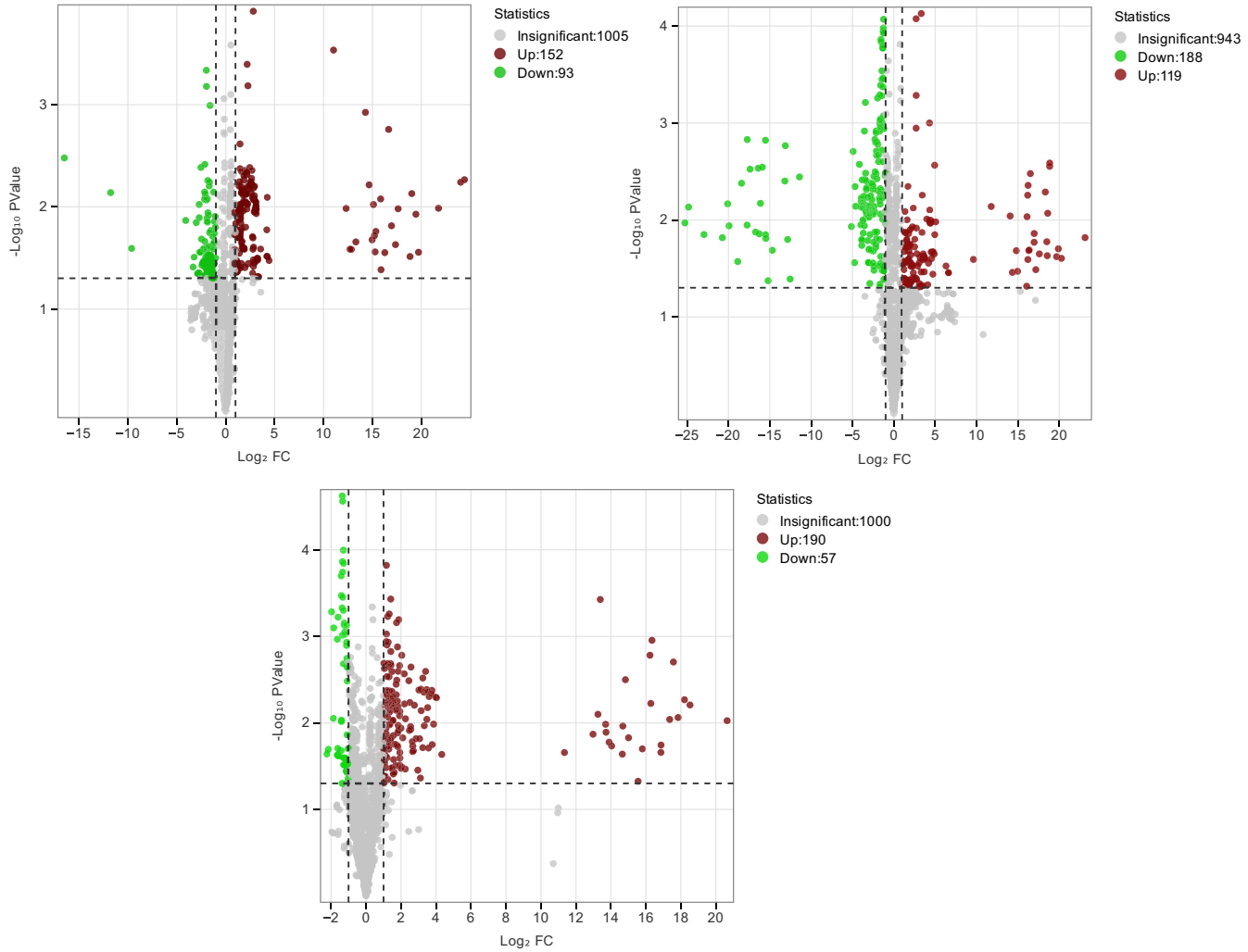

FIGURE 5 A Volcano plot of metabolites differentiation among different *Toona sinensis* morphs. Each dot represents a metabolite. Green dots represent down-regulated differential metabolites, red dots indicate up-regulated differential metabolites, and gray dots signify detected metabolites with no significant difference. The abscissa shows the logarithmic value (log2FC) of the relative content difference of a metabolite between the two sample groups. A larger absolute value on the abscissa indicates a greater relative content difference of the substance between the two groups. In the dual screening condition of VIP + FC, the ordinate represents the VIP value. A higher ordinate value indicates a more significant difference and a more reliable differential metabolite obtained by screening. In the triple filter condition of VIP + FC + P-value, the ordinate represents the significance level of the difference (-log10P-value), while the size of the dot corresponds to the VIP value.

1006 showed no significant change. Finally, in the R and G group, the expression of 119 metabolites was increased; 187 decreased; and 944 showed no significant changes (Figure 5).

The KEGG annotation was conducted on the identified metabolites to provide a comprehensive understanding of their biological functions and significance in various life processes. The KEGG

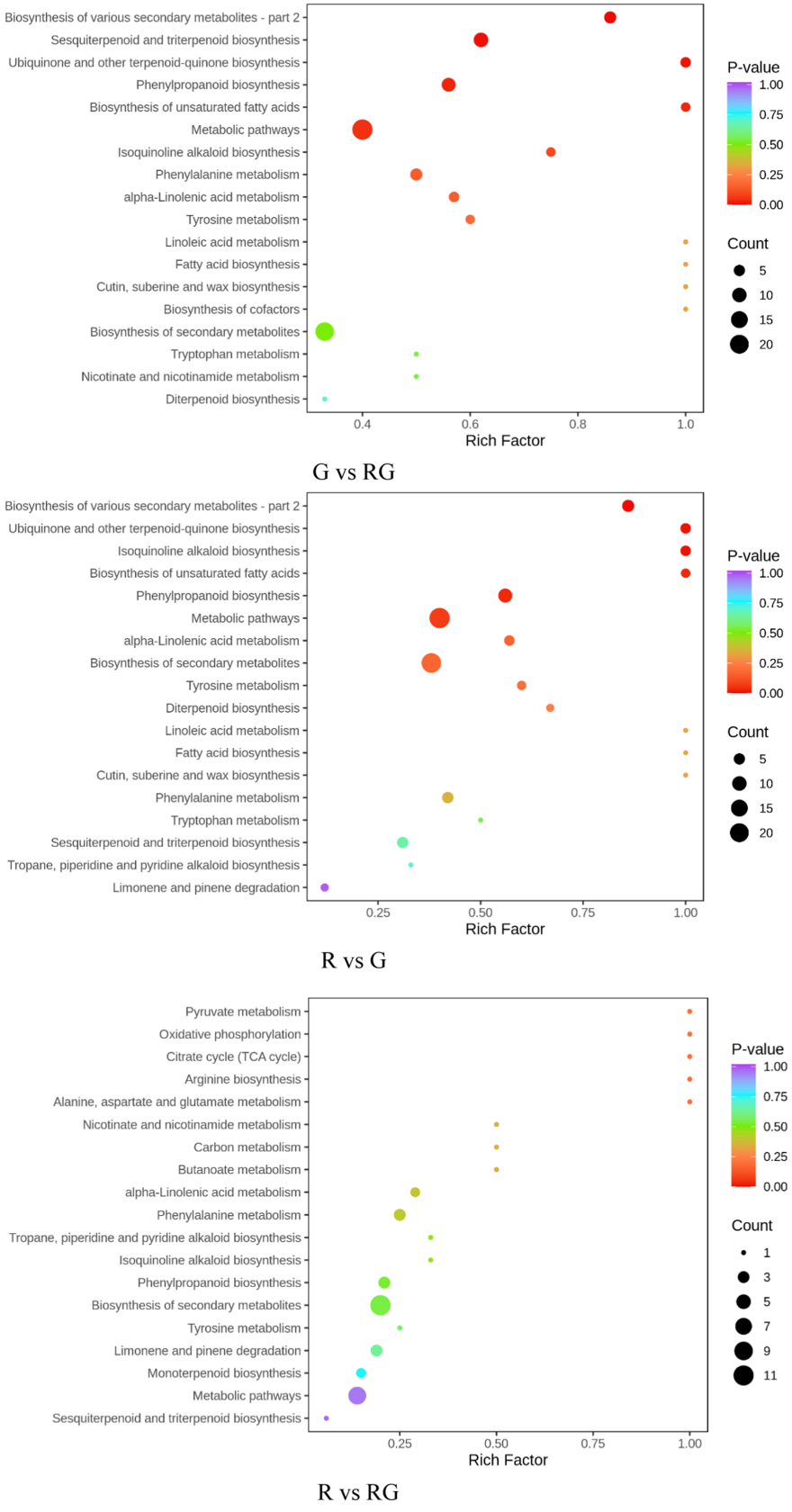

FIGURE 6 KEGG enrichment map of differential metabolites in different *Toona sinensis* morphs. The abscissa represents the Rich Factor corresponding to each pathway, while the ordinate displays the name of the pathway sorted by P-value. The color of the point reflects the size of the P-value, with a redder color indicating more significant enrichment. Additionally, the size of the dot represents the number of enriched differential metabolites.

database is a primary repository for pathway-related information, publicly accessible at http://www.genome.jp/kegg/. Functional annotation of all metabolites obtained from Toona samples revealed enrichment primarily in the following pathways: 'metabolic pathways', 'biosynthesis of secondary metabolites', 'sesquiterpenoid and triterpenoid biosynthesis', 'phenylalanine metabolism', 'isoquinoline alkaloid biosynthesis', 'alpha-Linolenic acid metabolism', and 'tyrosine metabolism' (Figure 6) among various Toon groups studied. *In vivo*, the interaction of multiple proteins orchestrates their biological functions. Hence, pathway-based annotation extends our comprehension of their biological roles even more profoundly.

3.2 | Clustering, transcriptome sequencing and functional enrichment of DEGs

To investigate the molecular regulatory mechanisms and variation of aroma-producing substances in different coloured *Toona sinensis* morphs, we conducted transcriptome sequencing on green leaves (G), red leaves with green stalks (RG), and fully red leaves (R). Following initial data filtration and error rate examination, a total of 4.21–5.91 million high-quality clean reads were obtained through an analysis of the GC content distribution (Table 1). Altogether, the nine transcriptome Toona samples (R, G and RG) yielded clean data of 64.99 Gb, averaging 6.31Gb/sample, with Q30 bases above 92.68%.

The differentially expressed genes (DEGs) were compared among the three *Toona sinensis* morphs. Across all samples, 14,339 total DEGs based on |log2Fold Change| ≥ 1 and FDR <0.05 using DESeq2/edgeR were detected. A total of 5563 DEGs (3026 upregulated and 2537 downregulated) between the R and RG group's transcriptome were connected. Collectively, 4282 DEGs (1852 upregulated and 2430 downregulated) between the R and G groups were harvested. However, 4494 DEGs in total (1763 upregulated and 2731 downregulated) between the G and RG group dissected out. Additionally, 252 common DEGs among the three groups were identified (Figure 7).

The expression data across different samples were centralized, standardized, and then clustered using K-means to analyze the expression patterns of the DEGs. In the K-mean analysis, the data was divided into two categories. There were many differentially expressed genes among three experimental treatments, which were classified into two categories: one for upregulation of genes and one for downregulation of genes. The DEGs in the leaves of different coloured Toon morphs were clustered into two subclasses based on their gene expression patterns. Subclasses 1 and 2 exhibited significant enrichment (Figure S2). Specifically, DEGs in subclass 2 exhibited upregulation, while those in subclass 1 showed downregulation.

To provide a comprehensive understanding of gene properties and functions, gene ontology (GO) was employed, categorizing genes and gene products into three components: biological process, cellular component, and molecular function. A total of Top 50 enriched GO terms was identified among groups (R_vs_RG, G_vs_RG, and R_vs_G).

TABLE 1 Transcriptome sequencing output statistics among different *Toona sinensis* morphs.

Sample	Raw Reads	Clean Reads	Clean Base (G)	Q30 (%)
R1	51028460	50117302	7.52	94.13
R2	44290452	43499370	6.52	93.01
R3	44351192	43250306	6.49	93.66
RG1	47047276	46251108	6.94	94.37
RG2	51780966	50943106	7.64	94.00
RG3	52878364	51972068	7.80	94.42
G1	43082866	42083696	6.31	92.68
G2	46764504	46086818	6.91	93.71
G3	59937864	59088554	8.86	93.93

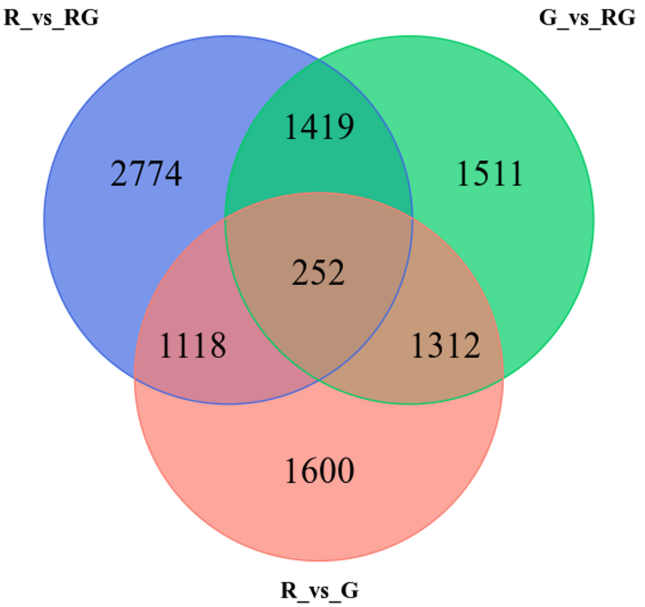

FIGURE 7 The differential expressed genes (DEGs) comparison among the three *Toona sinensis* morphs.

Biological process-related GO terms between the Toona group (G_vs_RG) indicated 34 distinct functions of differentially expressed genes. Particularly the biological process in plant-type cell wall biosynthesis (1.49%) and cell wall macromolecule metabolic process (1.41%). However, the molecular function of oxidoreductase activity (1.08%) was highly enriched in them.

The GO analysis of DEGs in the R_vs_G group revealed significant enrichment in cellular processes of a large ribosomal subunit (1.46%), biological function of cell wall macromolecule metabolic process (1.82%), and molecular function of oxidoreductase activity (1.14%). In the R_vs_RG group, the GO terms related to the biological process were enriched in 'cellular response to jasmonic acid stimulus (1.55%)', 'jasmonic acid-mediated signalling pathway (1.55%)' and 'regulation of innate immune response (1.55%)'. At the same time, the cellular component of the large ribosomal

FIGURE 8 The GO enrichment analysis of DEGs in *Toona sinensis* morphs.

subunit (1.38%) showed the most significant enrichment. Moreover, the molecular function of transcription corepressor activity (0.61%) was significantly enriched (Figure 8). The molecular function analysis indicated that most genes were involved in binding and catalytic activity while also contributing to an integral part of cell and cellular components.

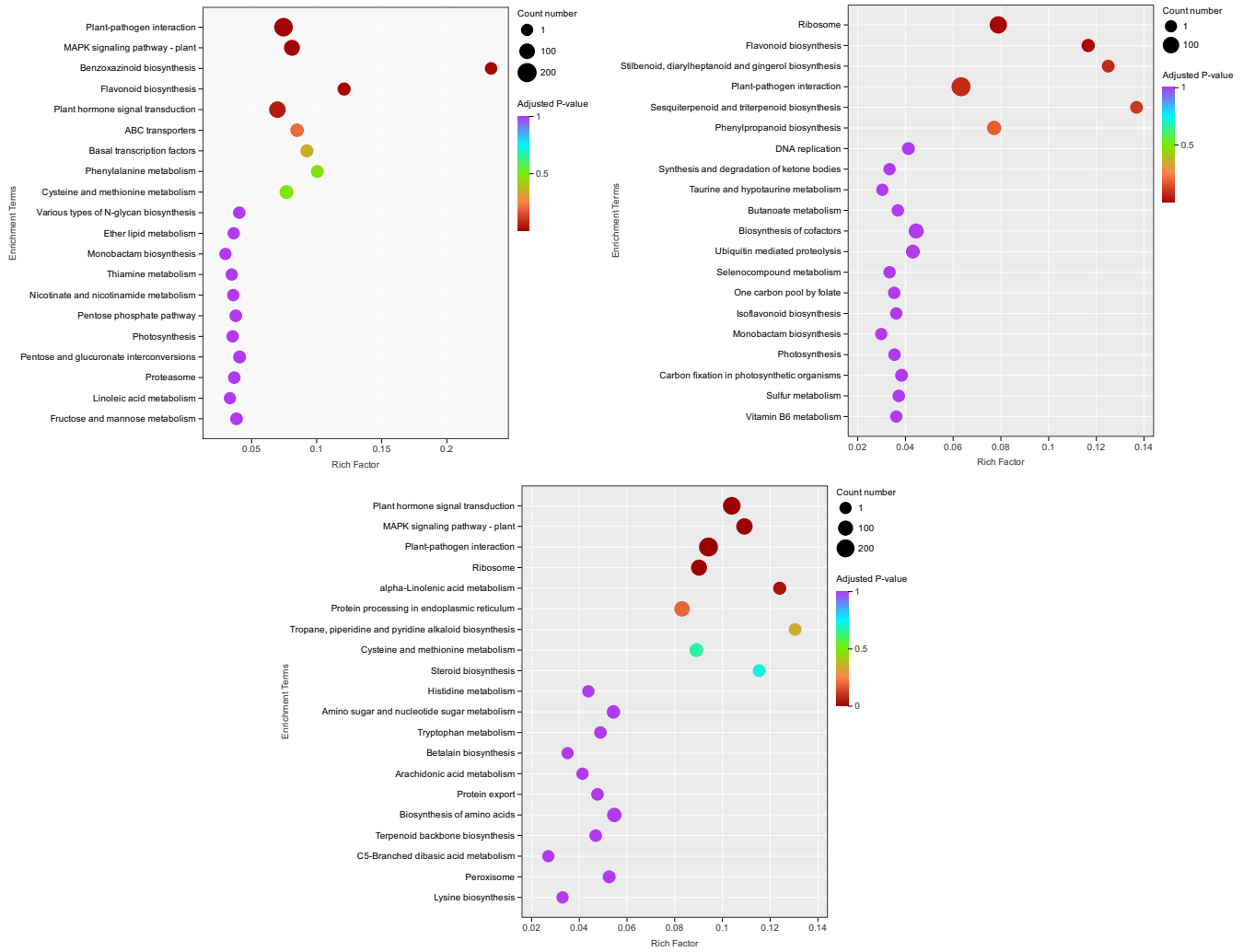

FIGURE 9 The KEGG pathway analysis indicative flavonoid and metabolites enrichment in *Toona sinensis* different morphs. The abscissa represents the Rich Factor corresponding to each pathway, while the ordinate displays the name of the pathway sorted by P-value. The color of the point reflects the size of the P-value, with a redder color indicating more significant enrichment. The size of the dot represents the number of enriched differential metabolites.

According to the results of KEGG metabolic analysis, disparities in the DEGs were illustrated while observing different coloured Toona groups. Primarily, the R_vs_RG group was observed, and the terms significantly enriched (q-value <0.05) were 'plant hormone signal transduction' (189 DEGs), 'MAPK signalling pathway- plant' (147 DEGs), 'plant-pathogen interaction' (235 DEGs), and 'ribosome' (136 DEGs). Later, the R_vs_G group indicated an "enrichment of' ribosomes" (119 DEGs), 'Plant pathogen interaction' (115 DEGs), and 'flavonoid biosynthesis' (26 DEGs). Meanwhile, observing G_vs_RG group's metabolic analysis, it was found that four pathways were significantly enriched: 'plant-pathogen interaction' (186 DEGs), 'plant hormone signal transduction' (127 DEGs), 'MAPK signalling pathway – plant' (109 DEGs), 'flavonoid biosynthesis' (27 DEGs), and 'benzoxazinoid biosynthesis' (11 DEGs). These findings shed light on the metabolic processes underlying the colouring differences in *Toona sinensis*. Differences in the expression of genes in the flavonoid biosynthesis pathway primarily account for the variation in colour between green and red *Toona sinensis* (Figure 9).

3.3 | Identification of co-expressed gene networks and key candidates

When the transcriptome data was coupled in the WGCNA module with FPKM values, 84 distinct gene modules were identified based on the co-expression pattern of individual genes. These gene modules are labelled in distinct colours and presented as a cluster dendrogram and network heatmap (Figure 10a, b). Notably, the brown module contained genes related to phenylpropanoid biosynthesis. These genes exhibited a negative correlation with green *Toona sinensis* (G) and red leaves with green stems genotypes (RG), but a positive correlation with red genotypes (R). In addition, the blue module (13 genes) and the steel blue module (5 genes) exhibited a

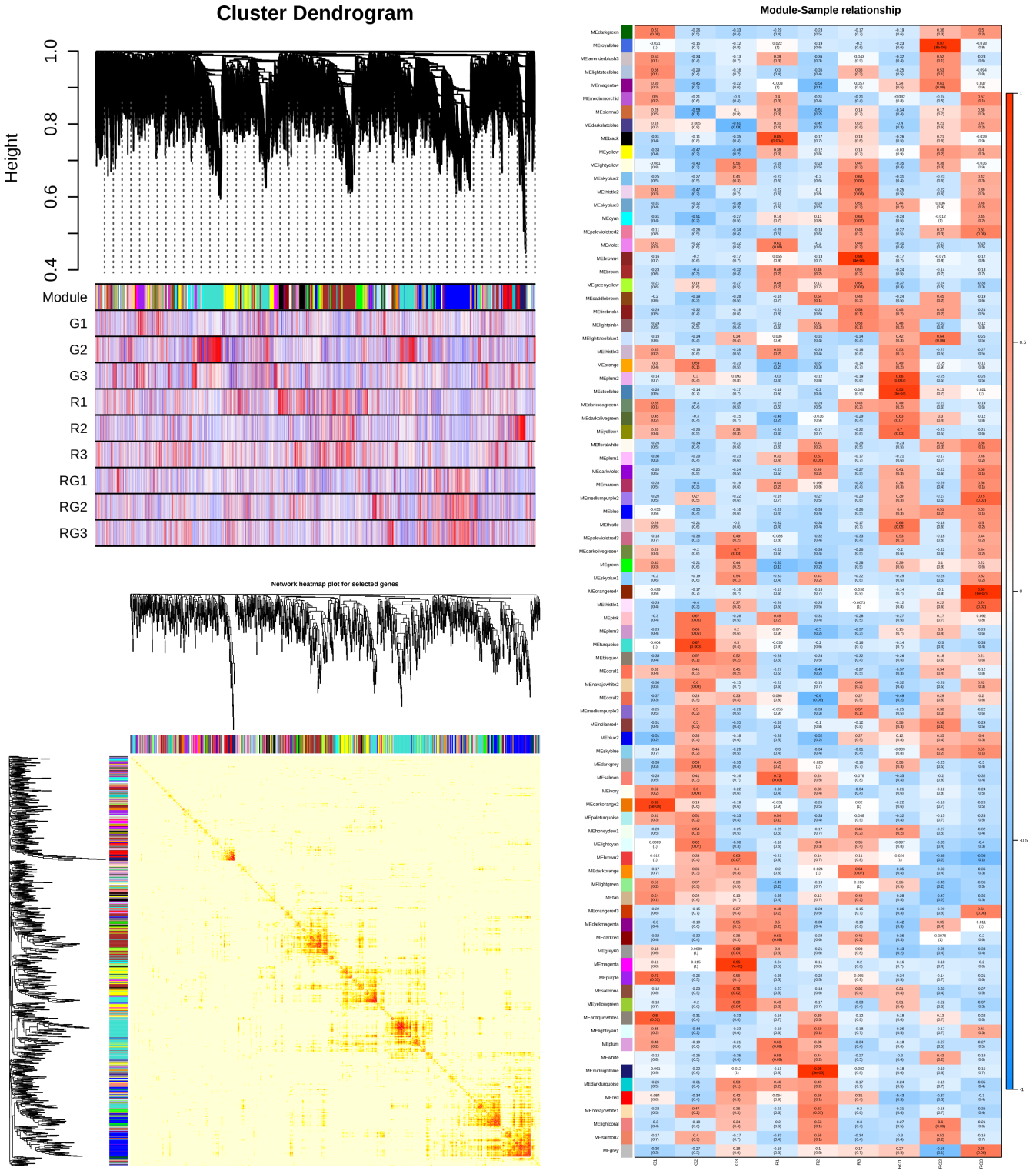

FIGURE 10 The Transcriptome data coupled in the WGCNA module with FPKM values. A- Cluster Dendrogram, B- Network heatmap plot for selected genes, C- Module sample relationship.

predominant concentration of genes related to terpenoid synthesis. These modules displayed a positive correlation with red leaves with green stems *Toona sinensis* (RG) and a negative correlation with green genotypes (G) and red genotypes (R) (Figure 10c). These results highlight differences in the synthesis of secondary metabolites among green (G), red (R), and red leaves with green stems (RG) *Toona sinensis*. Differences in aroma components among green (G), red (R), and red leaves with green stems (RG) *Toona sinensis* morphs may primarily stem from variations in the expression patterns of genes associated with terpene synthesis and phenylpropanoid biosynthesis.

3.4 | Integrated metabolomic and transcriptomic analysis

The metabolic and transcriptomic PCA data in *Toona sinensis* revealed significant differences among the morphs (Figure 3). Simultaneous DEGs and KEGG differential metabolites enrichment in the three morphs (R_vs_RG, R_vs_G, and G_vs_RG), disclosed the pathways enriched included 'phenylpropanoid biosynthesis' (R_vs_RG: 41 DEGs and 3 metabolites; G_vs_RG: 45 DEGs and 9 metabolites; R_vs_G: 49 DEGs and 9 metabolites), 'metabolic pathways' (R_vs_RG: 775 DEGs and 8 metabolites; G_vs_RG: 649 DEGs and 24 metabolites; R_vs_G: 651 DEGs and 24 metabolites), and 'biosynthesis of secondary metabolites' (R_vs_RG: 428 DEGs and 11 metabolites; G_vs_RG: 385 DEGs and 19 metabolites; R_vs_G: 342 DEGs and 22 metabolites).

Using the 'Cor' package in R, Pearson's correlation coefficients (PCCs) were computed for the DEGs and differential metabolites within each group. A comprehensive set of 680 DEGs and 257 metabolites were identified for R_vs_RG, 1512 DEGs and 431 metabolites for R_vs_G, and 136 DEGs and 64 metabolites for G_vs_RG. Leveraging all these DEGs and metabolites, we constructed a robust two-way orthogonal partial least squares (O2PLS) model. Through meticulous assessment of high-correlation variables and their weights across different datasets via loading diagrams, we successfully pinpointed key variables significantly influencing each omics dataset. Decisively, 10 metabolites, including five terpenoids, one heterocyclic compound, one phenol, one ketone, one aldehyde, and one alcohol (Figure 11). Many DEGs in different colours of *Toona sinensis* were related to the synthesis of terpenoids, which is also the metabolic pathway responsible for the aroma differences between different colours of *Toona sinensis*. However, the colour difference between green and red *Toona sinensis* was due to differences in gene expression in the flavonoid biosynthesis pathway.

Additionally, fifteen genes exhibited high expression levels and were significantly affected by the biosynthesis of secondary metabolites, sesquiterpenoid, phenylpropanoid biosynthesis, and triterpenoid biosynthesis in coloured *Toona sinensis* morphs. The synthesis of terpene metabolites predominantly occurs through the terpene metabolic pathway, which involves the activity of eight crucial gene families. These genes were labeled as *cluster-2071.59959*, *cluster-2071.50716*, *cluster-2071.13725*, *cluster-2071.88910*, *cluster-2071.105822*, *cluster-2071.62032*, *cluster-2071.96340*, *cluster-2071.101442*, *cluster-2071.115471*, *cluster-2071.32887*, *cluster-2071.4557*, *cluster-2071.44425*, *cluster-2071.44426*, *cluster-2071.30328*, *and cluster-2071.111438*.

3.5 | Combined analysis of transcriptomics and metabolomics provides insights into mechanisms of terpenoid biosynthesis

To understand the differences in terpenoid synthesis in the leaves of the three differently coloured *Toona sinensis*, transcriptomics and metabolomics data were integrated for analysis. Diterpenoid biosynthesis pathways included sclareol, (1R, 4aR, 4bR, 10aR)-7-Isopropyl-1,4a-dimethyl-1,2,3,4,4a,4b,5,6,10,10a-decahydrophenanthrene-1-carbaldehyde, Sesquiterpenoid and triterpenoid biosynthesis pathways included (Z)-1-Methyl-4-(6-methylhept-5-en-2-ylidene)cyclohex-1-ene, Germacrene D, δ- cadinene, (1R, 4R, 4aS, 8aR)-4,7-Dimethyl-1-(prop-1-en-2-yl)-1,2,3,4,4a,5,6,8a-octahydronaphthalene, geosmin, d-Nerolidol, 1,6,10-Dodecatriene, 7,11-dimethyl-3-methylene-, Limonene and pinene degradation pathways included 1-Cyclohexene-1-carboxylic acid, 4-(1-methylethenyl)-, (−)-Myrtenol, Bicyclo

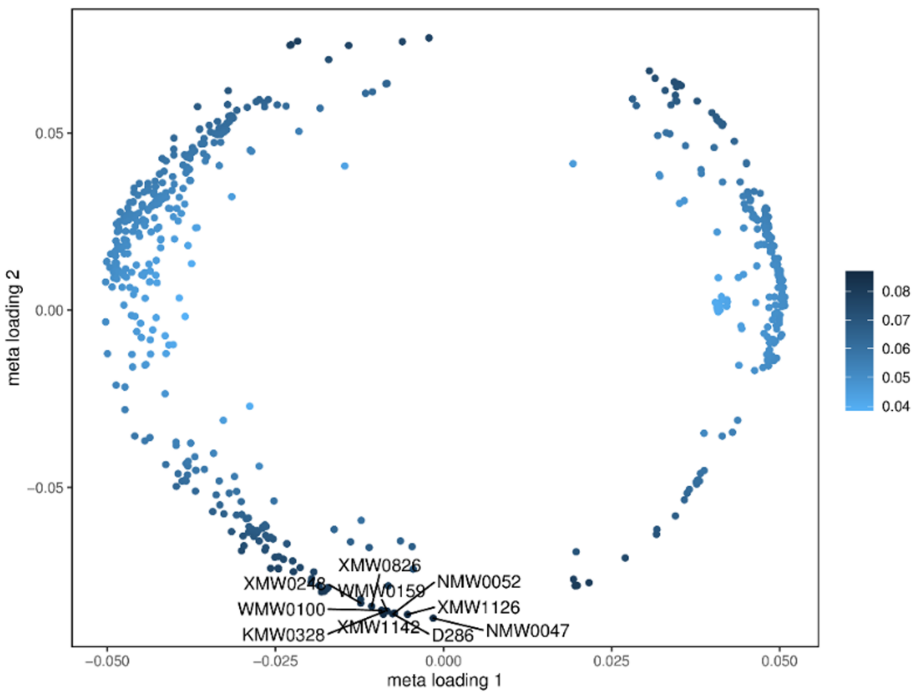

FIGURE 11 The PCCs of the DEGs and top 10 differential metabolites.

TABLE 2 Correlation analysis between differentially expressed genes (DEGs) and differentially expressed metabolites (DEMs).

Gene ID	KEGG	Compound	Pearson's correlation coefficients
Cluster-2071.115474	K13070 (EC:1.1.1.295)	1-Naphthalenepropanol, α-ethenyldecahydro-2-hydroxy-α,2,5,5,8a-pentamethyl-, [1R-[1.α.(R*),2.β.,4a.β.,8a.α.]]-(sclareol)	0.95
		(1R, 4aR,4bR, 10aR)-7-Isopropyl-1,4a-dimethyl-1,2,3,4,4a,4b,5,6,10,10a-decahydrophenanthrene-1-carbaldehyde	0.85
Cluster-2071.60851	K17961 (EC:1.14.14.58 1.14.14.59)	1-Naphthalenepropanol, α.-ethenyldecahydro-2-hydroxy-.α.,2,5,5,8a-pentamethyl-, [1R-[1.α.(R*),2.β.,4a.β.,8a.α.]]-(sclareol)	0.89
Cluster-2071.69169	K04125 (EC:1.14.11.13)	1-Naphthalenepropanol, α.-ethenyldecahydro-2-hydroxy-.α.,2,5,5,8a-pentamethyl-, [1R-[1.α.(R*),2.β.,4a.β.,8a.α.]]-(sclareol)	−0.95
Cluster-2071.91633	K04125 (EC:1.14.11.13)	1-Naphthalenepropanol, α.-ethenyldecahydro-2-hydroxy-.α.,2,5,5,8a-pentamethyl-, [1R-[1.α.(R*),2.β.,4a.β.,8a.α.]]-(sclareol)	0.94
Cluster-2071.46001	K15803 (EC:4.2.3.75)	(Z)-1-Methyl-4-(6-methylhept-5-en-2-ylidene) cyclohex-1-ene	0.81
		Naphthalene, 1,2,3,5,6,8a-hexahydro-4,7-dimethyl-1-(1-methylethyl)-, (1S-cis)-(δ- cadinene)	−0.88
		(1R, 4R, 4aS, 8aR)-4,7-Dimethyl-1-(prop-1-en-2-yl)-1,2,3,4,4a,5,6,8a-octahydronaphthalene	−0.83
		d-Nerolidol	−0.81
Cluster-2071.84751	K04125 (EC:1.14.11.13)	1-Naphthalenepropanol, α.-ethenyldecahydro-2-hydroxy-.α.,2,5,5,8a-pentamethyl-, [1R-[1.α.(R*),2.β.,4a.β.,8a.α.]]-(sclareol)	0.85
		(1R, 4aR, 4bR, 10aR)-7-Isopropyl-1,4a-dimethyl-1,2,3,4,4a,4b,5,6,10,10a-decahydrophenanthrene-1-carbaldehyde	0.87
Cluster-2071.87505	K04125 (EC:1.14.11.13)	(1R, 4aR, 4bR, 10aR)-7-Isopropyl-1,4a-dimethyl-1,2,3,4,4a,4b,5,6,10,10a-decahydrophenanthrene-1-carbaldehyde	−0.83
Cluster-2071.117931	K00511 (EC:1.14.14.17)	(Z)-1-Methyl-4-(6-methylhept-5-en-2-ylidene)cyclohex-1-ene	0.81
Cluster-2071.18222	K00511 (EC:1.14.14.17)	(Z)-1-Methyl-4-(6-methylhept-5-en-2-ylidene)cyclohex-1-ene	0.91
		Naphthalene, 1,2,3,5,6,8a-hexahydro-4,7-dimethyl-1-(1-methylethyl)-, (1S-cis)-(δ- cadinene)	−0.90
		(1R, 4R, 4aS, 8aR)-4,7-Dimethyl-1-(prop-1-en-2-yl)-1,2,3,4,4a,5,6,8a-octahydronaphthalene	−0.95
		d-Nerolidol	−0.85
		1,6,10-Dodecatriene, 7,11-dimethyl-3-methylene-	−0.87
Cluster-2071.3682	K15803 (EC:4.2.3.75)	(Z)-1-Methyl-4-(6-methylhept-5-en-2-ylidene)cyclohex-1-ene	−0.93
Cluster-2071.13725	K14173 (EC:4.2.3.46)	(1R, 4R, 4aS, 8aR)-4,7-Dimethyl-1-(prop-1-en-2-yl)-1,2,3,4,4a,5,6,8a-octahydronaphthalene	0.82
		d-Nerolidol	0.82
Cluster-2071.115548	K00511 (EC:1.14.14.17)	Germacrene D	−0.81
		Naphthalene, 1,2,3,5,6,8a-hexahydro-4,7-dimethyl-1-(1-methylethyl)-, (1S-cis)-	−0.88
		(1R, 4R, 4aS, 8aR)-4,7-Dimethyl-1-(prop-1-en-2-yl)-1,2,3,4,4a,5,6,8a-octahydronaphthalene	−0.83
		4a(2H)-Naphthalenol, octahydro-4,8a-dimethyl-, (4.α, 4a.α, 8a.β.)-(geosmin)	−0.80
		d-Nerolidol	−0.81
Cluster-2071.59959	K15472 (EC:1.14.14.151)	(Z)-1-Methyl-4-(6-methylhept-5-en-2-ylidene)cyclohex-1-ene	0.95
		Naphthalene, 1,2,3,5,6,8a-hexahydro-4,7-dimethyl-1-(1-methylethyl)-, (1S-cis)-(δ- cadinene)	−0.86
		(1R, 4R, 4aS, 8aR)-4,7-Dimethyl-1-(prop-1-en-2-yl)-1,2,3,4,4a,5,6,8a-octahydronaphthalene	−0.92
		d-Nerolidol	−0.81

(Continues)

TABLE 2 (Continued)

Gene ID	KEGG	Compound	Pearson's correlation coefficients
Cluster-2071.49632	K00128 (EC:1.2.1.3)	1-Cyclohexene-1-carboxylic acid, 4-(1-methylethenyl)-	0.98
		(−)-Myrtenol	−0.82
Cluster-2071.47260	K00128 (EC:1.2.1.3)	Bicyclo[3.1.1]heptan-3-ol, 6,6-dimethyl-2-methylene-	0.87
		Bicyclo[3.1.1]heptan-3-ol, 6,6-dimethyl-2-methylene-, [1S-(1.α.,3.α.,5.α.)]-	0.86

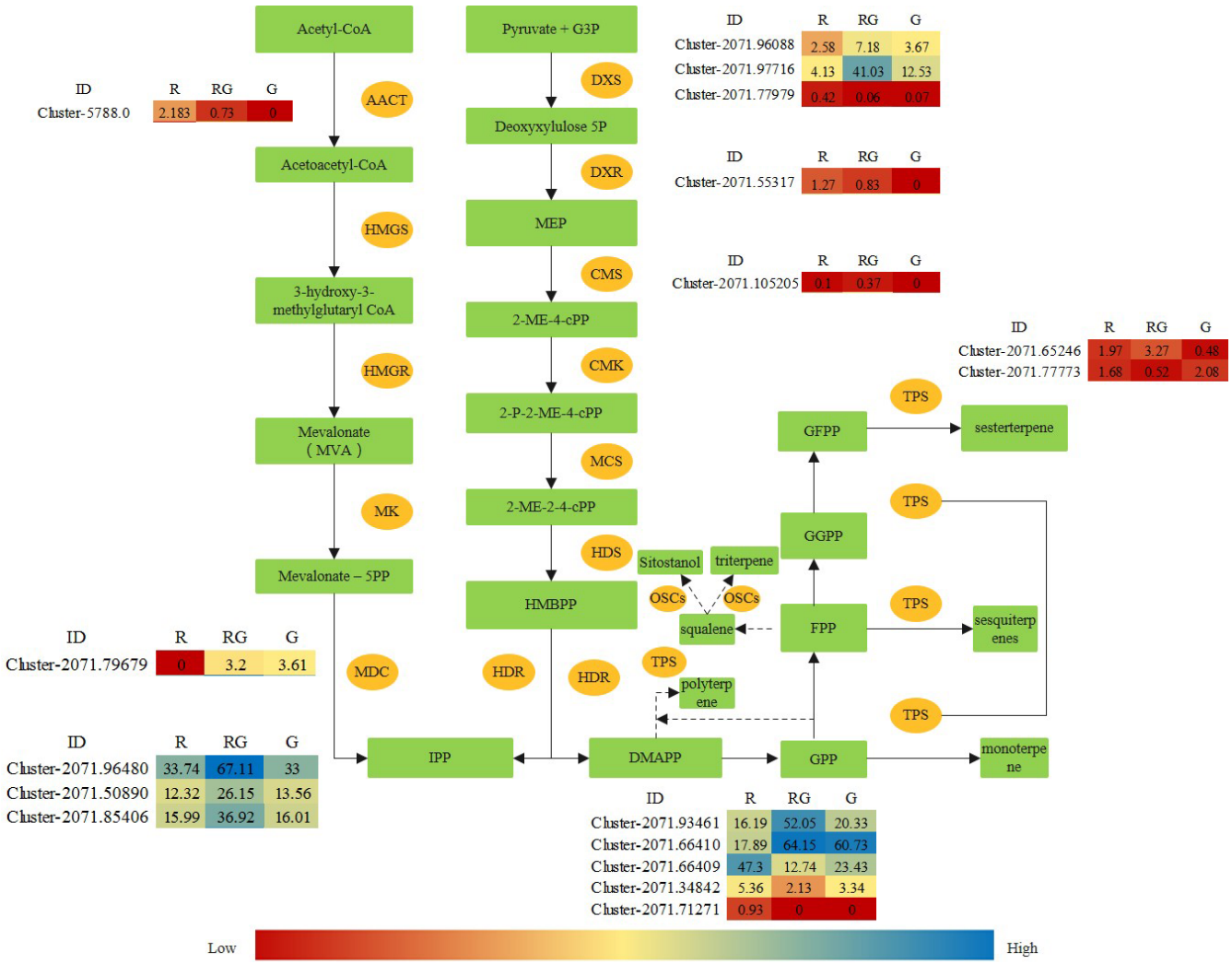

FIGURE 12 The proposed pathway of converting top 10 metabolites into flavonoids.

[3.1.1]heptan-3-ol, 6,6-dimethyl-2-methylene-, Bicyclo[3.1.1]heptan-3-ol, 6,6-dimethyl-2-methylene-, [1S-(1.α.,3.α.,5.α.)]- as a DEM. (Table 2). A total of 67 significant DEGs were found to be enriched in terpenoid synthesis pathways based on combined enrichment analysis, including 34 DEGs in the sesquiterpenoid and triterpenoid biosynthesis pathway, 20 DEGs in the diterpenoid biosynthesis pathway, and 13 DEGs in the limonene and pinene degradation pathway.

Terpene metabolites are mainly produced by the terpene metabolic pathway (Figure 12), the synthesis of terpenes occurs primarily through the mevalonate (MVA) and 2-C-methyl-D-erythritol-4-phosphate (MEP) pathways (Pu et al. 2021).

4 | DISCUSSION

The present study provides a comprehensive analysis of the genetic and metabolic mechanisms underlying the phenotypic variations observed in different coloured *Toona sinensis* morphs. The

phenological behaviours and environmental conditions could elevate the photosynthesis and intercellular CO_2 in Toona morph, especially in their intraseasonal growth and anatomical properties (Heinrich & Banks, 2006). Using transcriptomic and metabolomic approaches, we explored how differential gene expression influences the biosynthesis of key metabolites, particularly those involved in flavonoid and terpenoid pathways, which in turn dictate the colouration and aroma of these plants. A large number of DEGs were related to terpenoid synthesis, which is the metabolic pathway that underlies the aroma difference between green and red *Toona sinensis*. Furthermore, the difference in colour between green and red *Toona sinensis* is due mainly to differences in gene expression in the flavonoid biosynthesis pathway (Figure 9). The terpenoids, esters, heterocyclic compounds, ketones, alcohols, and hydrocarbons were found earlier to be involved in several biosynthesis pathways (Jiang et al., 2022).

The molecular mechanisms underlying the colour variation in *Toona sinensis* are intricately linked to differences in gene expression, particularly within the flavonoid biosynthesis pathway. Our comprehensive analysis revealed a significant number of DEGs between the green, red, and red-green variants, with a notable concentration in pathways associated with secondary metabolite biosynthesis, including phenylpropanoids and terpenoids. This differential gene expression likely drives the production of distinct pigments, resulting in the observed colour differences (Smith 2020). The clustering of DEGs into distinct modules, such as the blue and steel blue modules, highlights the coordinated regulation of terpenoid synthesis, further emphasizing the complexity of metabolic regulation in these plants (Jones, 2019). Additionally, the integration of metabolomic data using the O2PLS model provided insight into the correlation between transcriptomic and metabolomic changes, underscoring the significant impact of specific metabolites, including terpenoids, phenols, and flavonoids, on the overall phenotypic expression (Wang, 2021). These findings collectively suggest that the differences in gene expression profiles, particularly in the flavonoid biosynthesis pathway, play a crucial role in defining the colour and potentially the aromatic properties of *Toona sinensis* varieties.

4.1 | Gene Expression and Flavonoid Biosynthesis

Both flavonoids and terpenoids are important secondary metabolites that play key roles in the plant's defence mechanisms, growth, and development. One of the key findings of this study is the significant role of the flavonoid biosynthesis pathway in determining the colour differences between green, red, and red-green *Toona sinensis* varieties. Flavonoids are crucial pigments that contribute to plant colouration by producing a wide range of hues, from yellow to red (Tanaka et al., 2008). While flavonoids and terpenoids are biosynthesized through distinct pathways, our study suggests that both pathways share biosynthetic precursors and are often influenced by common intermediates. Indeed, both phenylpropanoids (which give rise to flavonoids) and isoprenoids (which give rise to terpenoids) originate from primary metabolites like acetyl-CoA, malonyl-CoA, and phenylalanine. This means that the availability of these precursors could potentially influence the production of both types of metabolites. For example, a shift in the flux of carbon from phenylalanine (which is used in the synthesis of flavonoids) could impact the availability of acetyl-CoA, which is also a precursor for the mevalonate pathway leading to terpenoid biosynthesis (Figure 12). The high enrichment of flavone, flavonol and flavonoid biosynthesis in green and red-green Toona morphs (G_Vs_RG and R_Vs_G) indicated the potential impact of the flavonoid pathway in colouration across the three *Toona sinensis* varieties. (Figure 9). This increased expression likely results in higher flavonol content, contributing to the green colouration observed in the green (G) and red-green (RG) varieties. These findings align with previous research that has highlighted the role of flavonoids in plant pigmentation, particularly in species where colour variation is a prominent phenotypic trait (Petroni & Tonelli, 2011).

The upregulation of genes within the flavonoid biosynthesis pathway suggests a tightly regulated mechanism that controls the synthesis and accumulation of these pigments. Such regulation could be influenced by both genetic factors and environmental cues, which together shape the final phenotype. The involvement of specific transcription factors that regulate the expression of flavonoid biosynthetic genes could be a potential area of further research, as these factors have been shown to play critical roles in the pigmentation of other plant species (Grotewold, 2006).

4.2 | Terpenoid Synthesis and Aroma

In addition to colour, the aroma of *Toona sinensis* is a distinguishing characteristic that varies between the different coloured varieties. Terpenoids, which are synthesized through the terpenoid metabolic pathway, are primary contributors to plant aroma and have been extensively studied for their role in producing volatile organic compounds (VOCs) that define the scent profile of plants (Pichersky & Raguso, 2018). Our study identified significant differences in the expression of genes related to terpenoid synthesis, with these genes predominantly clustered in the blue and steel-blue modules. These modules exhibited differential expression patterns across the green, red, and red-green *Toona sinensis* varieties, suggesting that the variation in aroma is largely driven by the differential expression of terpenoid-related genes. A similar conclusion was made by Zhang et al. (2023) for the aroma variation of plum fruits. Modules related to phenylpropanoid biosynthesis (Savoi et al., 2016) and terpenoid synthesis (Anwar et al., 2021) are particularly noteworthy, as they are known to contribute to pigmentation and aroma (Yeon & Kim, 2021).

The integration of transcriptomic data with metabolomic profiles further supported the role of terpenoids in determining the aromatic properties of *Toona sinensis*. The O2PLS model analysis revealed that terpenoids were among the top metabolites affected by transcriptomic changes, with several key terpenoid compounds showing strong correlations with specific gene expression patterns (Figure 11). This indicates that the regulation of terpenoid biosynthesis is closely linked to the expression of specific genes, which could be targeted in future

breeding programs aimed at enhancing or modifying the aromatic qualities of *Toona sinensis*.

4.3 | Phenylpropanoid Biosynthesis and Secondary Metabolite Production

The phenylpropanoid pathway is another crucial metabolic pathway identified in this study, which is involved in the biosynthesis of a wide range of secondary metabolites, including flavonoids, lignins, and coumarins (Vogt, 2010). Our results showed that genes involved in phenylpropanoid biosynthesis were differentially expressed across the different *Toona sinensis* varieties, with the highest expression levels observed in the red variety. This differential expression likely contributes to the accumulation of various secondary metabolites that not only affect colour and aroma but also play roles in plant defence and stress responses.

The significant enrichment of phenylpropanoid-related genes in the red variety suggests a potential link between colour and the production of secondary metabolites. Previous studies have demonstrated that red pigmentation in plants is often associated with increased levels of phenolic compounds, which are products of the phenylpropanoid pathway and are known for their antioxidant properties (Fraser & Chapple, 2011). These compounds may provide additional protective benefits to the red *Toona sinensis* variety, potentially contributing to its ecological fitness and adaptation to specific environmental conditions.

4.4 | Integration of Transcriptomics and Metabolomics

The integration of transcriptomic and metabolomic data in this study provided a holistic view of the metabolic networks underlying the phenotypic diversity in *Toona sinensis*. The establishment of a two-way orthogonal partial least squares (O2PLS) model facilitates the identification of highly correlated variables across datasets, the key metabolites and genes influencing the differences (Zhang et al., 2023). By using the O2PLS model, we were able to identify key metabolites and genes that are tightly correlated, providing insights into how changes in gene expression can lead to alterations in metabolite production and, consequently, phenotypic traits such as colour and aroma. Pathways such as phenylpropanoid biosynthesis, metabolic pathways, and biosynthesis of secondary metabolites were significantly enriched, indicating their importance in determining colour variation and aroma composition (Guo et al., 2019). One of the most striking findings from this integrative analysis was the identification of specific terpenoids and phenolic compounds that were highly correlated with gene expression patterns associated with flavonoid and terpenoid biosynthesis. These metabolites are likely critical determinants of the observed phenotypic differences, and their identification opens up new avenues for targeted breeding and genetic modification to enhance desirable traits in *Toona sinensis* (Sumner et al., 2015). Understanding the molecular regulatory mechanisms underlying these traits can facilitate targeted breeding strategies and quality regulation practices. Overall, the study contributes to a better understanding of the complex interplay between gene expression, metabolite composition, and phenotype in *Toona sinensis*, paving the way for future research and applications in agriculture, horticulture, and functional food development.

5 | CONCLUSION

In summary, our study provides valuable insights into the molecular mechanisms underlying the phenotypic diversity in *Toona sinensis*. *Toona sinensis* exhibits a diverse range of metabolites, including terpenoids, esters, and phenolic compounds. A total of 1251 metabolites were identified, encompassing terpenes (22.56%) and esters (16.72%), contributing to the flavour, aroma, and nutritional properties of the plant. Copaene terpenoid was high in red (R) Toona morph, L-α-terpineol in red-green and α-ionone in green. The differential expression of genes involved in flavonoid and terpenoid biosynthesis plays a central role in determining the colour and aroma of different *Toona sinensis* morphs. The transcriptome samples (R, G and RG) yielded clean data of 64.99Gb, averaging 6.31Gb/sample, with Q30 bases above 92.68%. Conclusively, 10 metabolites, including five terpenoids, one heterocyclic compound, one phenol, one ketone, one aldehyde, and one alcohol, were highly attributed. Fifteen genes exhibited high expression levels and were significantly affected by the phenylpropanoid biosynthesis. The secondary metabolites may influence the physiological response to environmental conditions in various Toona morphs, further emphasizing the ecological significance of the identified pathways. The integration of transcriptomic and metabolomic data has revealed key metabolites and gene networks that contribute to these phenotypic traits, offering potential targets for future breeding and genetic improvement efforts.

AUTHORSHIP CONTRIBUTION STATEMENT

RZ conceived the project and designed the experiments; RZ, MZ and YG performed the experiments; RZ, and MUF analyzed the data; RZ, JA, MUF and JH were major contributors in writing the manuscript; RZ was involved in funding acquisition; SL, XL, SIA and SS reviewed and edited the manuscript; all authors discussed the results and reviewed the manuscript.

SUPPLEMENTARY INFORMATION

A supplementary file with additional data is attached.

ACKNOWLEDGEMENTS

The authors would like to acknowledge Chengdu Normal University for support and assistance in experiments. Open access publishing facilitated by The University of Western Australia, as part of the Wiley - The University of Western Australia agreement via the Council of Australian University Librarians.

FUNDING INFORMATION

This research was funded by the High-Level Talent Introduction Program of Chengdu Normal University (YJRC2021-03), Teaching Reform Project of Chengdu Normal University(2023JG19), Sichuan Provincial Key Laboratory of Philosophy and Social Sciences for Monitoring and Evaluation of Rural Land Utilization (NDZDSB2023004) Sichuan Provincial Key Laboratory for Development and Utilization of Characteristic Horticultural Biological Resources (TSYY202403). Figure 7 was obtained within the state assignment of Ministry of Science and Higher Education of the Russian Federation (theme No. 122050400128–1).

DATA AVAILABILITY STATEMENT

All data are included in the manuscript.

DECLARATION OF INTERESTS

The authors declare that they have no known competing interest.

COMPLETE ETHICAL STATEMENT

Not Applicable.

ORCID

Suleyman I. Allakhverdiev https://orcid.org/0000-0002-0452-232X
Sergey Shabala https://orcid.org/0000-0003-2345-8981

REFERENCES

Anwar, M., Chen, L., Xiao, Y., Wu, J., Zeng, L., Li, H., Wu, Q. & Hu, Z. (2021) Recent advanced metabolic and genetic engineering of phenylpropanoid biosynthetic pathways. *International Journal of Molecular Sciences*, 22(17), 9544

Borges, R.M., Bessiere, J.M. & Ranganathan, Y. (2013) Diel variation in fig volatiles across syconium development: making sense of scents. *Journal of Chemical Ecology*, 39(5), 630–642

Chen, C.J., Michaelis, M., Hsu, H.K., Tsai, C.C., Yang, K.D., Wu, Y.C., Cinatl, J., Jr. & Doerr, H.W. (2008) *Toona sinensis* Roem tender leaf extract inhibits SARS coronavirus replication. *Journal of Ethnopharmacology*, 120(1), 108–111

Chen, Y., Bonkowski, M., Shen, Y., Griffiths, B.S., Jiang, Y., Wang, X. & Sun, B. (2020) Root ethylene mediates rhizosphere microbial community reconstruction when chemically detecting cyanide produced by neighbouring plants. *Microbiome*, 8(1), 4

Du, F., Wang, T., Fan, J.M., Liu, Z.Z., Zong, J.X., Fan, W.X., Han, Y.H. & Grierson, D. (2019) Volatile composition and classification of lilium flower aroma types and identification, polymorphisms, and alternative splicing of their monoterpene synthase genes. *Horticulture Research*, 6(1), 110

Dudareva, N., Klempien, A., Muhlemann, J.K. & Kaplan, I. (2013) Biosynthesis, function and metabolic engineering of plant volatile organic compounds. *New Phytologist*, 198(1), 16–32

Fei, X., Qi, Y., Lei, Y., Wang, S., Hu, H. & Wei, A. (2021) Transcriptome and metabolome dynamics explain aroma differences between green and red prickly ash fruit. *Foods*, 10(2)

Fraser, C.M. & Chapple, C. (2011) The phenylpropanoid pathway in arabidopsis. *The Arabidopsis Book/American Society of Plant Biologists*, *9*

Grotewold, E. (2006) The genetics and biochemistry of floral pigments. *Annual Review of Plant Biology*, 57(1), 761–780

Guo, Y., Zhu, C., Zhao, S., Zhang, S., Wang, W., Fu, H., Li, X., Zhou, C., Chen, L. & Lin, Y. (2019) De novo transcriptome and phytochemical analyses reveal differentially expressed genes and characteristic secondary metabolites in the original oolong tea (Camellia sinensis) cultivar 'Tieguanyin'compared with cultivar 'Benshan'. *BMC Genomics*, 20(1), 1–24

Heinrich, I. & Banks, J.C., 2006. Variation in phenology, growth, and wood anatomy of *Toona sinensis* and *Toona ciliata* in relation to different environmental conditions. *International Journal of Plant Sciences* 167(1), 831–841.

Holopainen, J.K. & Gershenzon, J. (2010) Multiple stress factors and the emission of plant VOCs. *Trends in Plant Science*, 15(3), 176–184

Ji, Y.T., Xiu, Z., Chen, C.H., Wang, Y., Yang, J.X., Sui, J.J., Jiang, S.J., Wang, P., Yue, S.Y., Zhang, Q.Q., Jin, J.L., Wang, G.S., Wei, Q.Q., Wei, B., Wang, J., Zhang, H.L., Zhang, Q.Y., Liu, J., Liu, C.J., Jian, J.B. & Qu, C.Q. (2021) Long read sequencing of *Toona sinensis* (A. Juss) roem: A chromosome-level reference genome for the family meliaceae. *Molecular Ecology Resources*, 21(4), 1243–1255

Jiang, H.U., Jia-Xun, L.I., Qiang, L.I., Tian-Feng, P., Xiao-Dong, S., Tao, L., Jian, C., Nian-Hua, J., Wei-Xing, Y. & Wei, W. (2020) Terpenoids from *Toona sinensis*. *Zhongguo Zhong Yao Za Zhi*, 45(18), 4411–4415

Jiang, M., Lan, S., Wang, Z., Pu, X. & Zhuang, L. (2022) Analysis of the volatile components in different parts of three ferula species via combined DHSA-GC-MS and multivariate statistical analysis. *LWT - Food Science and Technology*, 167(1), 113846

Jiang, X., Zhang, B., Lei, M., Zhang, J. & Zhang, J. (2019) Analysis of nutrient composition and antioxidant characteristics in the tender shoots of Chinese toon picked under different conditions. *LWT - Food Science and Technology*, 109(1), 137–144

Jones, A. (2019) Gene clustering and pathway regulation in secondary metabolite synthesis. *Plant Science Today*, 14(4), 89–102

Kalske, A., Shiojiri, K., Uesugi, A., Sakata, Y., Morrell, K. & Kessler, A. (2019) Insect herbivory selects for volatile-mediated plant-plant communication. *Current Biology*, 29(18), 3128–3133 e3123

Langfelder, P. & Horvath, S. (2008) WGCNA: an R package for weighted correlation network analysis. *BMC Bioinformatics*, 9(1), 559

Lim, H.J., Park, I.S., Jie, E.Y., Ahn, W.S., Kim, S.J., Jeong, S.I., Yu, K.Y., Kim, S.W. & Jung, C.H. (2020) Anti-Inflammatory activities of an extract of In vitro grown adventitious shoots of *Toona sinensis* in LPS-treated RAW264.7 and propionibacterium acnes-treated HaCaT cells. *Plants (Basel)*, 9 (12)

Liu, C., Zhang, J., Zhou, Z., Hua, Z., Wan, H., Xie, Y., Wang, Z. & Deng, L. (2013) Analysis of volatile compounds and identification of characteristic aroma components of *Toona sinensis*(A. Juss.) roem. using GC-MS and GC-O. *Food and Nutrition Sciences*, 4(3), 305–314

Pei, G., Chen, L. & Zhang, W. (2017) WGCNA application to proteomic and metabolomic data analysis. *Methods in Enzymology*, 585(1), 135–158

Peng, W., Liu, Y., Hu, M., Zhang, M., Yang, J., Liang, F., Huang, Q. & Wu, C. (2019) *Toona sinensis*: a comprehensive review on its traditional usages, phytochemisty, pharmacology and toxicology. *Revista Brasileira de Farmacognosia*, 29(1), 111–124

Petit Bon, M., Böhner, H., Kaino, S., Moe, T. & Bråthen, K.A. (2020) One leaf for all: chemical traits of single leaves measured at the leaf surface using near-infrared reflectance spectroscopy. *Methods in Ecology and Evolution* 11(1), 1061–1071.

Petroni, K. & Tonelli, C. (2011) Recent advances on the regulation of anthocyanin synthesis in reproductive organs. *Plant Science*, 181(3), 219–229

Pichersky, E. & Raguso, R.A. (2018) Why do plants produce so many terpenoid compounds? *New Phytologist*, 220(3), 692–702

Pu, X., Dong, X., Li, Q., Chen, Z. & Liu, L. (2021) An update on the function and regulation of methylerythritol phosphate and mevalonate pathways and their evolutionary dynamics. *Journal of Integrative Plant Biology*, 63(7), 1211–1226

Savoi, S., Wong, D.C., Arapitsas, P., Miculan, M., Bucchetti, B., Peterlunger, E., Fait, A., Mattivi, F. & Castellarin, S.D. (2016) Transcriptome and metabolite profiling reveals that prolonged drought modulates the phenylpropanoid and terpenoid pathway in white grapes (Vitis vinifera L.). *BMC Plant Biology*, 16(1), 1–17

Smith, J. (2020) The role of flavonoid pathway in plant pigmentation. *Journal of Plant Biology*, 45(2), 123–135

Song, X., Wang, J., Li, N., Yu, J., Meng, F., Wei, C., Liu, C., Chen, W., Nie, F., Zhang, Z., Gong, K., Li, X., Hu, J., Yang, Q., Li, Y., Li, C., Feng, S., Guo, H., Yuan, J., Pei, Q., Yu, T., Kang, X., Zhao, W., Lei, T., Sun, P., Wang, L., Ge, W., Guo, D., Duan, X., Shen, S., Cui, C., Yu, Y., Xie, Y., Zhang, J., Hou, Y., Wang, J., Wang, J., Li, X.Q., Paterson, A.H. & Wang, X. (2020) Deciphering the high-quality genome sequence of coriander that causes controversial feelings. *Plant Biotechnology Journal*, 18(6), 1444–1456

Sumner, L.W., Lei, Z., Nikolau, B.J. & Saito, K. (2015) Modern plant metabolomics: advanced natural product gene discoveries, improved technologies, and future prospects. *Natural Product Reports*, 32(2), 212–229

Tanaka, Y., Sasaki, N. & Ohmiya, A. (2008) Biosynthesis of plant pigments: anthocyanins, betalains and carotenoids. *The Plant Journal*, 54(4), 733–749

Vogt, T. (2010) Phenylpropanoid biosynthesis. *Molecular Plant*, 3(1), 2–20

Wang, H., Hua, J., Yu, Q., Li, J., Wang, J., Deng, Y., Yuan, H. & Jiang, Y. (2021) Widely targeted metabolomic analysis reveals dynamic changes in non-volatile and volatile metabolites during green tea processing. *Food Chemistry*, 363(1), 130131

Wang, L. (2021) Metabolomic and transcriptomic integration in plant secondary metabolism. o*Omics: A Journal of Integrative Biology*, 25(3), 205–216

Wei, G., Tian, P., Zhang, F., Qin, H., Miao, H., Chen, Q., Hu, Z., Cao, L., Wang, M., Gu, X., Huang, S., Chen, M. & Wang, G. (2016) Integrative analyses of nontargeted volatile profiling and transcriptome data provide molecular insight into VOC diversity in cucumber plants (*Cucumis sativus*). *Plant Physiology*, 172(1), 603–618

Wu, J.G., Peng, W., Yi, J., Wu, Y.B., Chen, T.Q., Wong, K.H. & Wu, J.Z. (2014) Chemical composition, antimicrobial activity against *Staphylococcus aureus* and a pro-apoptotic effect in SGC-7901 of the essential oil from *Toona sinensis* (A. Juss.) roem. leaves. *Journal of Ethnopharmacology*, 154(1), 198–205

Xia, Z., Huang, D., Zhang, S., Wang, W., Ma, F., Wu, B., Xu, Y., Xu, B., Chen, D., Zou, M., Xu, H., Zhou, X., Zhan, R. & Song, S. (2021) Chromosome-scale genome assembly provides insights into the evolution and flavor synthesis of passion fruit (*Passiflora edulis Sims*). *Horticulture Research*, 8(1), 14

Yang, H.L., Chen, S.C., Lin, K.Y., Wang, M.T., Chen, Y.C., Huang, H.C., Cho, H.J., Wang, L., Kumar, K.J. & Hseu, Y.C. (2011) Antioxidant activities of aqueous leaf extracts of *Toona sinensis* on free radical-induced endothelial cell damage. *Journal of Ethnopharmacology*, 137(1), 669–680

Yang, J., Ren, Y., Zhang, D., Chen, X., Huang, J., Xu, Y., Aucapina, C.B., Zhang, Y. & Miao, Y. (2021) Transcriptome-based WGCNA analysis reveals regulated metabolite fluxes between floral color and scent in *Narcissus tazetta* Flower. *International Journal of Molecular Sciences*, 22(15)

Yeon, J.Y. & Kim, W.S. (2021) Biosynthetic linkage between the color and scent of flowers: a review. *Horticultural Science and Technology*, 39(6), 697–713

Yu, W.J., Chang, C.C., Kuo, T.F., Tsai, T.C. & Chang, S.J. (2012) *Toona sinensis* roem leaf extracts improve antioxidant activity in the liver of rats under oxidative stress. *Food and Chemical Toxicology*, 50(6), 1860–1865

Zhai, X. (2020) *Characterization of the key aroma compounds in raw Toona sinensis (A. Juss.) roem. buds and their products by application of the molecular sensory science concept*. Technische Universität München,

Zhang, Q., Zhu, S., Lin, X., Peng, J., Luo, D., Wan, X., Zhang, Y., Dong, X. & Ma, Y. (2023) Analysis of volatile compounds in different varieties of plum fruits based on headspace solid-phase microextraction-gas chromatography-mass spectrometry technique. *Horticulturae*, *9*(10), 1069

Zhao, Q., Zhong, X.-L., Zhu, S.-H., Wang, K., Tan, G.-F., Meng, P.-H. & Zhang, J. (2022) Research advances in *Toona sinensis*, a traditional chinese medicinal plant and popular vegetable in China. *Diversity*, 14(7), 572

Zhou, C., Zhu, C., Tian, C., Xu, K., Huang, L., Shi, B., Lai, Z., Lin, Y. & Guo, Y. (2022) Integrated volatile metabolome, multi-flux full-length sequencing, and transcriptome analyses provide insights into the aroma formation of postharvest jasmine (*Jasminum sambac*) during flowering. *Postharvest Biology and Technology*, 183

SUPPORTING INFORMATION

Additional supporting information can be found online in the Supporting Information section at the end of this article.

How to cite this article: Zeng, R., Zheng, M., Gao, Y., Hu, J., Ahmad, J., Farooq, M.U. et al. (2025) Differential gene expression and metabolic pathways in *Toona sinensis*: Influence on colour and aroma. *Physiologia Plantarum*, 177(2), e70146. Available from: https://doi.org/10.1111/ppl.70146